SPIE's Proceedings, Volume 4980, Reliability, Testing, and Characterization of MEMS/MOEMS, San Jose, CA, January, 2003, pp 220 -228.

Resonant frequency method for monitoring MEMS fabrication

Danelle M. Tanner[∇], Albert C. Owen, Jr.[§], and Fredd Rodriguez
Sandia National Laboratories

ABSTRACT

MEMS surface-micromachining fabrication requires the use of many different tools to deposit thin-films, precisely define patterns using typical photolithography, and perform etching processes. As with any fabrication process there is inherent variation, which is acceptable when controlled within suitable limits. The ability to monitor and respond to this variation is paramount in maintaining a viable fabrication process. Electrostatic comb-drive resonators are candidate test structures used to validate uniformity in the MEMS fabrication process. Although directly dependent on mass and spring constant, a measure of their resonant frequencies generally provides a good indicator of both process repeatability and geometric variation.

In this study, sets of five graduated comb-drive resonator structures, located at each die on a ¼ wafer, were stimulated to resonant frequency using the "blur envelope" technique. This technique facilitates fast, straightforward, and repeatable resonant frequency measurements usually with a resolution of approximately 50-100 Hz. Wafer maps of resonant frequency versus die position for a ¼ wafer reveal a pattern with comb-drive resonator devices exhibiting highest resonant frequencies at the center and lowest at the perimeter of the wafer. Using a numerical model, coupled with discrete geometric measurements, a method was developed which links resonant frequency to fabrication parameters.

KEYWORD LIST

Comb-drive resonator, monitoring tool, resonant frequency measurement, parametric testing tool

NOMENCLATURE

ω_0	Resonant Frequency (Hz)	L	Spring Length (μm)
E	Youngs Modulus of Elasticity (Pa)	w	Spring Width (μm)
I	Moment of Inertia (μm^4)	t	Layer Thickness (μm)
F	Force (N)	K	Spring Constant
M_{eff}	Effective Resonator Mass (kg)	K_{eff}	Effective Spring Constant
A_{eff}	Effective Resonator Area (μm^2)	ρ	Density (kg/m^3)
V	Voltage (Volts)	R_s	Sheet Resistance (Ohms/square)
I	Current (Ohms)	n	Number of Comparisons Made
x	Calculated Spring Width (μm)	y	Measured Linewidth (μm)

[∇] Contact Info: tannerdm@sandia.gov; phone 505-844-8973; fax 505-844-2991; http://www.mems.sandia.gov; Sandia National Laboratories, PO Box 5800 MS-1081, Albuquerque, NM, USA 87185-1081

[§] Currently at the University of Colorado at Boulder

1. INTRODUCTION

Electrostatic comb-drive structures are common surface-micromachined devices typically employed as microelectromechanical systems actuators. In some cases, however, they can instead be effectively utilized as test devices for validating the MEMS fabrication process. A measure of their sensitive resonant frequencies generally provides a good indicator of device functionality, process repeatability, and geometric variation. By fabricating comb-drive resonators at each die on a wafer, measuring their resonant frequencies, and then comparing their measured values, it is possible to reveal such non-uniformities. The resonant frequency of a comb-drive resonator is directly dependant on its spring constant and mass. Therefore, changes in its resonant frequency can be mathematically linked to changes in its geometry. Figure 1a is a scanning electron microscope (SEM) image of a typical comb-drive resonator. Its movable central shuttle mass is supported by two sets of bifold springs. Applying a voltage at L or R will force the center mass towards the fixed electrostatic comb fingers. The underlying surface is grounded. The schematic given in Figure 1b labels the critical dimensions and components of the comb-drive resonator.

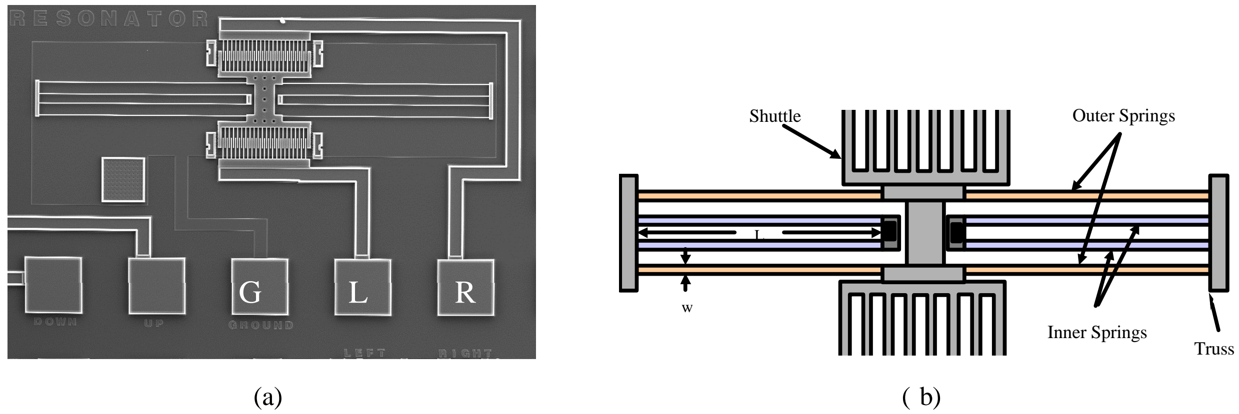

(a) (b)

Figure 1. (a) Scanning electron microscope image of a typical comb-drive resonator. (b) A schematic of a typical resonator displaying the moving shuttle, inner and outer sets of resonator springs, and critical dimensions, L and w.

2. REPRESENTATIVE MODEL

A mathematical model was derived to predict the undampened resonant frequency of the comb-drive resonators. Resonant frequency (ω) is directly dependent on mass and spring constant. Equation 1 demonstrates this relationship.

$$\omega_0 = \frac{1}{2\pi}\sqrt{\frac{K_{eff}}{M_{eff}}} \tag{1}$$

The resonator springs are composed of eight coupled springs with identical rectangular cross-sections. We can therefore use the beam deflection equation [1] for a perpendicularly loaded cantilever beam, with its free end allowing no rotation (i.e. the slope of the beam at its free end equals zero), to derive the effective spring constant (K_{eff}). The maximum deflection relation for a single spring is given in Equation 2.

$$Deflection = Y_o = \frac{FL^3}{12EI} \tag{2}$$

Since the applied spring force (F) is equivalent to the product of spring deflection (Y_o) and spring stiffness constant (K), and the moment of inertia (I) for a beam of rectangular cross-section can be represented as given in Equation 3,

$$I = \frac{1}{12} t w^3 \quad (3)$$

then Equation 2 may be simplified and rewritten as given in Equation 4:

$$K = \frac{Etw^3}{L^3} \quad (4)$$

By separately summing, in series or parallel as required, the spring constants for the other seven springs, an effective spring constant is obtained as given in Equation 5.

$$K_{eff} = \frac{2Etw^3}{L^3} \quad (5)$$

The weight of the springs and trusses can account for as much as 4-5% of the resonant frequency value. The kinetic energy equivalence method [2,3] was employed to derive an effective mass parameter for the comb drive resonator system. Equation 6 represents the mass of the system for determining resonant frequency.

$$M_{eff} = M_{Shuttle} + \frac{12}{35} M_{Springs} + \frac{1}{4} M_{Truss} \quad (6)$$

Substitution of Equations 5 and 6 into Equation 1 yields the following relation. In Equation 7, it is important to note that the spring width, *w*, presents the dimension most sensitive to change. A slight change in the spring width dimension has a relatively large effect on the spring constant and therefore, resonant frequency. Also, note that layer thickness, t, has no effect on the resonant frequency since it may be factored out of K_{eff} and M_{eff} ($M_{eff} = \rho t A_{eff}$) and then canceled in the resonant frequency equation.

$$\omega_0 = \frac{1}{2\pi} \sqrt{\frac{Ew^3}{\rho L^3 \left(A_{shuttle} + \frac{12}{35} A_{Springs} + \frac{1}{4} A_{Truss} \right)}} \quad (7)$$

3. EXPERIMENTAL APPROACH

3.1 Test method

For this study, identical sets of five graduated comb-drive resonator structures (approximately 10-30 kHz in 5 kHz increments), located at each die on the quarter-wafer, were used. The structures had differing spring lengths of 235, 179, 148, 128, and 113 µm. Using Equation 7 these lengths yielded design resonant frequencies of approximately 10.0, 15.2, 20.4, 25.4, and 30.7 kHz, respectively. Note that the spring width used in the calculations was 1.7 µm, even though the design was 2 µm. This is a result of a process bias during which a combination of photolithography and etch undercut contribute to a narrowing of line width as great as 0.15 µm. By fabricating comb-drive resonators at each die on the wafer, as shown in Figure 2, measuring their resonant frequencies, and then comparing their measured values, it is possible to reveal variation as a function of position on the wafer. Since spring width presents the most critical dimension to geometric variation, electrical linewidth measurements were performed using a standard linewidth

structure. The actual comb-drive resonator spring width was not measured. However, the electrical linewidth is expected to relate linearly to the resonator spring width.

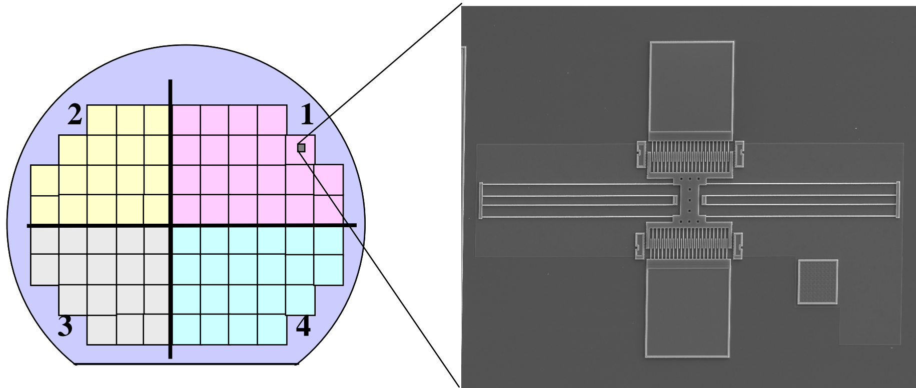

Figure 2. Schematic of a typical wafer bearing a comb-drive resonator at each of the 76 die locations. The wafer is separated into four quarters as designated.

3.2 Blur Envelope Method

To study the potential geometric variation on the wafer, comb-drive resonators were stimulated to resonant frequency using the "blur envelope" method. This technique facilitates fast, straightforward, and repeatable resonant frequency measurements usually with a resolution of about 50 –100 Hz. For this method, an adjustable electrical drive signal in the form of a sine wave is used to stimulate the comb drive resonator to resonant frequency. By holding the drive signal amplitude constant and carefully adjusting its frequency through a range where resonance is expected, the resonant frequency can be determined. The frequency, throughout this range, at which the comb drive resonator experiences the largest visual displacement, is the resonant frequency. Figure 3, courtesy of Tanner et al [4] illustrates the comb drive resonator before, at, and after achieving resonant frequency.

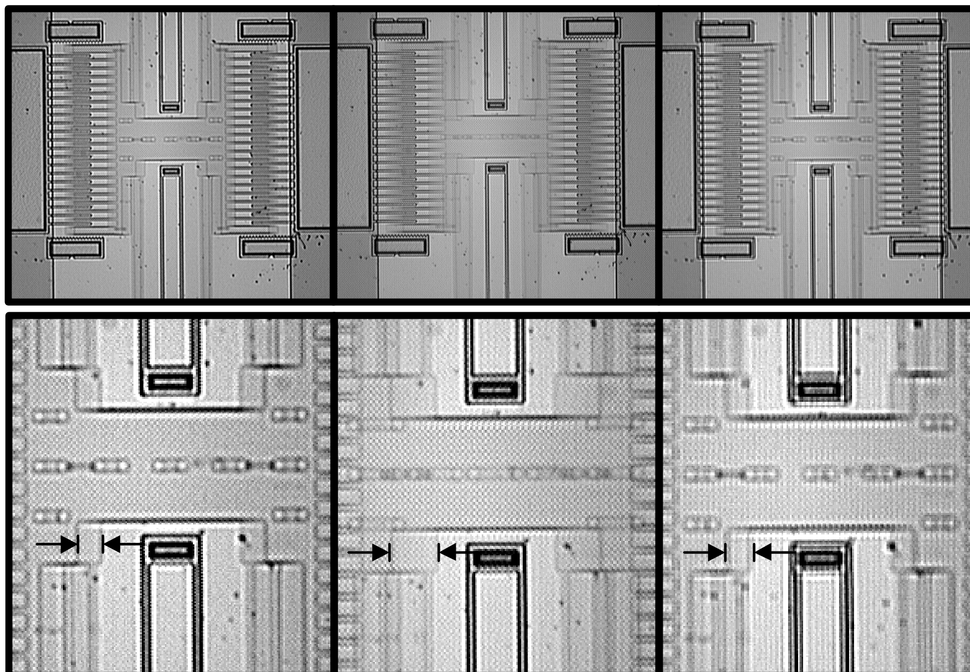

Figure 3. Before resonant frequency (left). At resonant frequency with maximum displacement (middle). After resonant frequency (right).

3.3 Linewidth measurement
Because the comb resonator spring width was somewhat difficult to measure, a separate test structure was used to examine linewidth as a function of position on the wafer. Theoretically, the linewidth should relate linearly to the spring width. The split-cross-bridge resistor structure, similar to that as given by Buehler and Hersey [5], was used to measure line width. In addition, the resistor is capable of electrically measuring line spacing, and line pitch. A general schematic of the split-cross-bridge resistor is given in Figure 4.

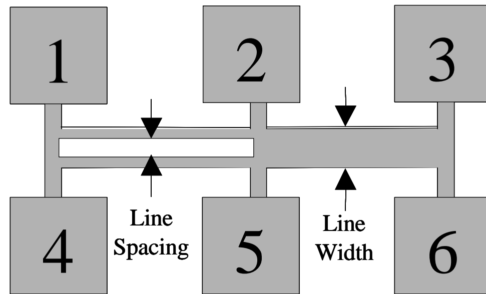

Figure 4. Split bridge cross resistor for measuring linewidth.

To measure electrical linewidth, a current of 1 mA was applied across contact pads 1 and 6 and the voltage drop was measured across contact pads 2 and 3. Next, to reduce measurement error the direction of the current was reversed and the voltage drop again measured. The voltage measurements were then averaged. Once the voltage drop and sheet resistance measurements were made at each die on the ¼ wafers, the linewidth was calculated using Equation 8 [5,6],

$$W_b = \frac{R_s L_{23} I_{16}}{V_{23}} \tag{8}$$

where the sheet resistance, R_s, was measured using a standard van der Pauw sheet resistance structure.

4. RESULTS AND DISCUSSION

4.1 Resonant frequency measurements
Wafer map plots of resonant frequency measurements versus die position for ¼ wafers reveal a trend with comb-drive resonator devices exhibiting highest resonant frequencies at the center and lowest resonant frequencies at the outermost perimeter of the wafer. Figure 5 illustrates the common pattern for the five different comb-drive resonators on a ¼ wafer dried using a hydrophobic self-assembled monolayer coating. In Figure 5 the center of the wafer piece is the lower left corner of each map. The data shown here are actual resonant frequency measurements. Grayscale shading has been used to group like results. Note that there is a radial dependence in the values, but the largest differences are seen on the edge die of the ¼ wafer. Due to the radial dependency of many fabrication processes (such as photoresist coat, develop, and plasma etch) edge die are well known to show the largest deviation from target.

Resonant Frequency

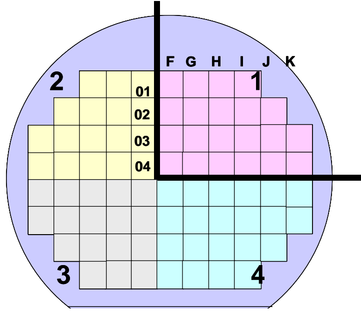

235 µm Spring Length

8.8	9.2	8.7			
10.2	10.2	9.8	9.3	7.5	
10.7	10.5	10	9.7	9.2	
10.7	10.7	10.4	10.4	9.9	8.1

179 µm Spring Length

13	12.8	11.9			
15.2	15.6	14.2	14		
16.1	16.2	15.3	14.6	13.9	
16.1	16.2	15.5	15.2	15.1	12.7

148 µm Spring Length

18.3	19.2				
21.2	21.6	19.8	18.6		
22.8	22	20.4	19.2	18.7	
21.8	21.7	20.8	20	19.5	17

128 µm Spring Length

23.2	24.1	23.3			
25.2	25.9	25.2	25.9		
27.4	29.0	28.9	26.0	23.6	22.9
28.1	27.0	26.0	25.2	24.1	

113 µm Spring Length

29.8	29.3	28.0			
32.7	32.9	31.8	29.0		
34.1	34.8	33.0	32.2	30.5	
34.6	34.3	33.8	34.1	32.2	

Figure 5. Wafer maps illustrating measured comb-drive resonant frequency variations on a ¼ wafer sample. The upper left diagram shows the area of the wafer probed for data (Quarter 1).

If we examine equation 7 and focus only on the width of the springs, we can determine the source of the trend. We assume that the cubic term in width dominates and ignore the linear width dependence of $A_{Springs}$. In that case, forming the ratio of resonant frequencies of springs with different widths yields the following equation:

$$\frac{\omega_{01}}{\omega_{02}} = \sqrt{\left(\frac{w_1}{w_2}\right)^3} \qquad (9)$$

If we use a typical width of 1.8 µm for a resonator, then a resonator with a more narrow width of only 0.1 µm would have a resonant frequency 92% lower. For a 0.2-µm difference in width, the resonant frequency would be 84% lower. As an example, a 30 KHz resonator would resonate at 25 KHz if only the width of the springs were narrowed by 0.2 µm.

4.2 Linewidth measurements

We used two techniques to investigate the linewidth effect; an electrical linewidth structure and actual measurement in the Scanning Electron Microscope (SEM). Much like the resonators, the linewidth measurements exhibit a similar pattern. The cross bridge resistor structures with the largest measured linewidth values tend to be near the center of the wafer. Correspondingly, the smallest measured linewidth values tend to be at the outermost perimeter of the wafer. The

edge dice tend to give rise to the largest differences. We had some difficultly with the electrical linewidth structure design of Figure 4. In our design, the split impinged into the bond-pad/line intersection, which could affect the resulting measurements. The calculated values are probably incorrect, but the relation between neighboring die should be reasonable. Figure 6 shows the wafer map for the electrical linewidth and SEM measurement. The design value was 8 μm so we believe the SEM values to be more accurate (resolution to ± 0.05 μm). It is typical for there to be a 0.3-μm undercut on beam widths due to a process bias during which a combination of photolithography and etch undercut contribute to a narrowing of line width as great as 0.15 μm per edge. Of course, this is a higher percentage effect for narrow beams.

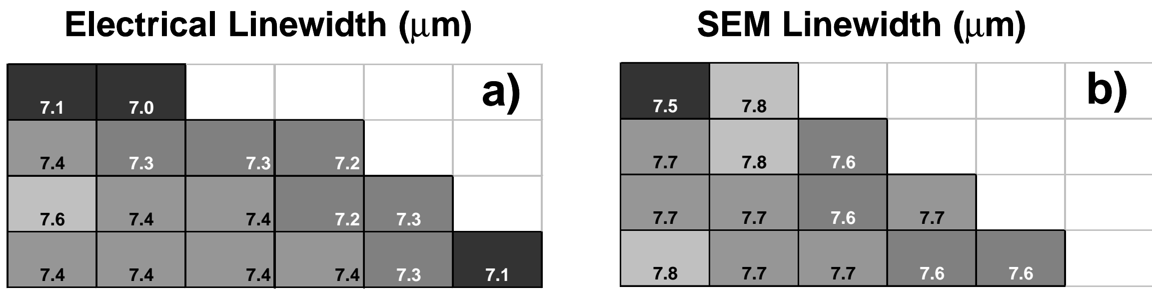

Figure 6. Linewidth measurement variations on a ¼ wafer sample using two techniques. The technique in a) used a typical electrical linewidth structure and in b) used the measurement capability of an SEM. The measurements are on an identical quarter using identical structures.

4.3 Method Comparison

There was a similarity between the measured resonant frequency and linewidth patterns across the ¼ wafer. To quantify the measurements technique agreement, we examined the measurements on a die-by-die basis. As shown in Equation 7, the spring width is a function of the resonant frequency, Young's modulus and the density of polysilicon, the length of the springs, and the effective area. This spring width was calculated for each comb-drive resonator (all 5 lengths) in each die on the quarter wafer. Because resonant frequency and length are inversely proportional in the equation, the calculated width should be the same for each length. The error in the resonator measurement was derived using standard propagation of error techniques and was dominated by the frequency error (± 100 Hz) and the error in Young's modulus (164.3 ± 3.2 GPa).[8] The Young's modulus error contributed to slightly more than half of the total error. The use of higher frequencies (shorter lengths) would minimize the effect of the frequency error ($\Delta L/L$), but the error in Young's modulus is fixed due to present measurement techniques.

The advantage of using five lengths is five separate measurements of the same value, linewidth. An average of all five predicted widths was performed and that width was normalized by a nominal width value. Additionally, all the SEM measurements were normalized by a nominal value and plotted in Figure 7, where the die location values are defined in Figure 5. All edge die and die without corresponding SEM linewidth measurements were not plotted.

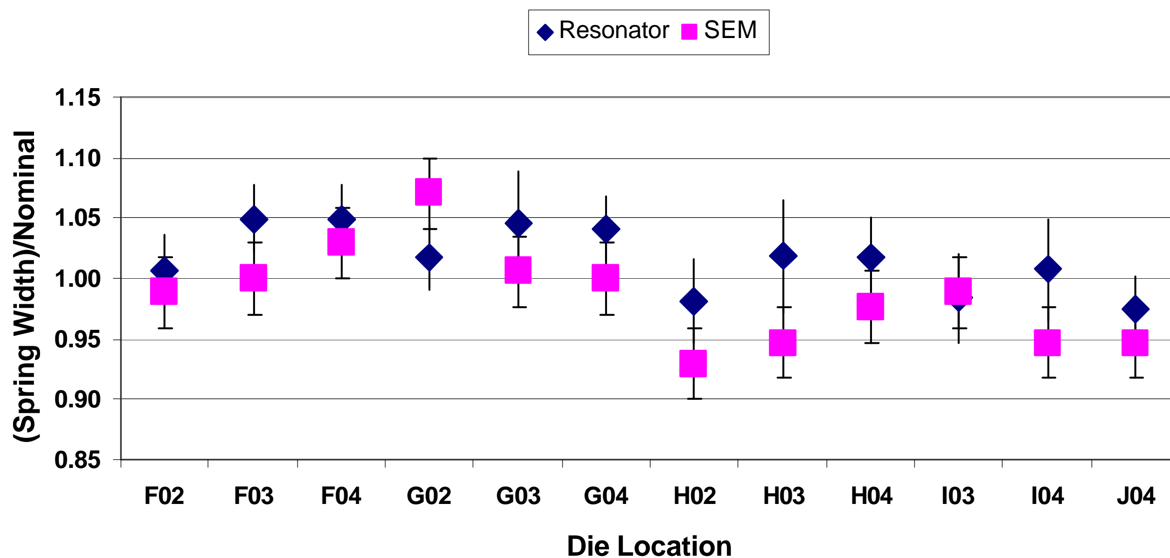

Figure 7. The agreement between the resonator and the SEM method for measuring linewidth is shown in this graph. Each resonator point is the average of five measurements corresponding to the five lengths. This demonstrates the excellent sensitivity of the resonator method. The die locations are defined in Figure 5.

The results not only show agreement between the resonator method and the SEM method, but also reveal that the sensitivity of the resonator method is equivalent to the SEM method. It would clearly be impractical to routinely measure linewidths using an SEM, but this resonator method could be implemented easily.

5. CONCLUSIONS

We have determined that the resonator method for measuring the fabrication parameter of linewidth has excellent sensitivity. This is due to the cubic spring-width dependence in the equation for resonant frequency. The comb-drive resonator resonant frequency and linewidth measurement patterns can be linked to several fabrication processes, including photoresist spin on, photoresist developing, and plasma etching, which may cause the radial variation phenomenon as seen in this study.

It is important to understand that geometric variation may not have an effect on devices operating at well below their resonant frequencies. However, for devices where adherence to strict dimensions is critical, the effect of linewidth variation should be minimized by designing devices to be less sensitive to linewidth variation. This can be done with the comb-drive resonator, for example, by increasing its spring width so that it is less sensitive to variation.

6. ACKNOWLEDGEMENTS

The authors thank the staff of the Microelectronics Development Laboratory (MDL) for fabrication, release, and technical expertise. The authors would also like to thank Sita Mani and Mike Baker for reviewing the report. We thank Jerry Walraven for the SEM measurements. We also thank Karen Helgesen, Guild Copeland, and Fred Sexton for their guidance and professionalism.

Sandia is a multiprogram laboratory operated by Sandia Corporation, a Lockheed Martin Company, for the United StatesDepartment of Energy under Contract DE-AC04-94AL85000.

7. REFERENCES

[1] R. J. Roark, *Formulas for Stress and Strain*, Chapter 8, McGraw-Hill Book Company, New York, 1965.

[2] C.W. De Silva, *Vibration: fundamentals and practice*, Chapter 2, CRC Press, Boca Raton, 2000.

[3] T. Mukherjee, S. Iyer, and G.K. Fedder, "Optimization-based synthesis of microresonators," Sensors and Actuators A, **Vol. 70**, pp. 118-127, 1998.

[4] D.M. Tanner et al, " MEMS Reliability: Infrastructure, Test Structures, Experiments, and Failure Modes," Sandia Report, SAND2000-0091, pp.31, 2000.

[5] M.G. Buehler and C.W. Hershey, " The split-cross-bridge resistor for measuring the sheet resistance, linewidth, and line spacing of conducting layers," IEEE Transactions on Electron Devices, **Vol. ED-33**, pp.1572-1579, 1986.

[6] D.K. Schroder, *Semiconductor Material And Device Characterization*, pp.9-14 and 487-489, John Wiley & Sons, New York, 1990.

[7] M.F. Triola, *Elementary Statistics*, pp.454, Addison-Wesley Publishing Company, Boston, 1992.

[8] B. D. Jensen, M. P. de Boer, N. D. Masters, F. Bitsie, and D. A. LaVan, "Interferometry of Actuated Microcantilevers to Determine Material Properties and Test Structure Nonidealities in MEMS," JMEMS, **10**, No.3, September 2001.